International Journal of Fluid Mechanics & Thermal Sciences
2015; 1(3): 54-58
Published online June 30, 2015 (http://www.sciencepublishinggroup.com/j/ijfmts)
doi: 10.11648/j.ijfmts.20150103.13

Fluid Dynamic Study of a NACA2415 Airfoil Type Wind Turbine with a Wedging Angle Equal to 30°

Tarek Chelbi[1], Zied Driss[1], Ahmed Kaffel[2], Mohamed Salah Abid[2]

[1]Laboratory of Electro-Mechanic Systems (LASEM), National School of Engineers of Sfax (ENIS), University of Sfax, Sfax, Tunisia
[2]Department of Mechanical Engineering, University of Maryland, College Park, Maryland, USA

Email address:

tarak.chelbi@gmail.com (T. Chelbi), zied.driss@enis.rnu.tn (Z. Driss), kaffel@umd.edu (A. Kaffel), MohamedSalah.Abid@enis.rnu.tn (M. S. Abid)

To cite this article:

Tarek Chelbi, Zied Driss, Ahmed Kaffel, Mohamed Salah Abid. Fluid Dynamic Study of a NACA2415 Airfoil Type Wind Turbine with a Wedging Angle Equal to 30°. *International Journal of Fluid Mechanics & Thermal Sciences*. Vol. 1, No. 3, 2015, pp. 54-58.
doi: 10.11648/j.ijfmts.20150103.13

Abstract: In this paper, numerical simulations and experimental validation were carried out to gain an insight into the complex flow field developing around a small wind rotor and to evaluate its performance. We consider the Navier-Stokes equations in conjunction with the standard k-ε turbulence model to study the aerodynamic parameters of a NACA2415 airfoil type wind turbine. These equations are solved numerically to determine the local characteristics of the flow and the models tested are implemented using the open source "SolidWorks Flow Simulation". Experiments have been also conducted on an open wind tunnel equipped by a small NACA2415 airfoil type wind turbine to validate the numerical results. This will help improving the aerodynamic efficiency in the design of packaged installations of the NACA2415 airfoil type wind turbine.

Keywords: NACA2415 Airfoil Wind Turbine, Wind Tunnel, Turbulent Flow, Aerodynamic Structure, CFD

1. Introduction

The increasing awareness of the general climate change and global warming has provided opportunities for wind turbine applications. For economic and technical reasons, wind energy is no longer well used. Although that clean energy finish, it appears blatantly that electricity contributes greatly to environmental degradation and the depletion of nonrenewable resources. Therefore, the steps to prepare a truly sustainable development are to increase the share of renewable resources for electricity generation. In this context, the production of electricity by wind turbines is playing a major role. A lot of scientists have experimentally and numerically examined the effects of such parameter design as blades number and airfoil profile. For example, Leifsson and Koziel [1] presented a transonic airfoil design optimization methodology that uses a computationally cheap, physics-based low-fidelity model to construct a surrogate of an accurate but CPU intensive high-fidelity model. The low-fidelity model, described by the transonic small-disturbance equation, is corrected by aligning its airfoil surface pressure distribution with the corresponding distribution of the high-fidelity model. Strinath and Mittal [2] utilized a continuous adjoint method for the design of airfoils in unsteady viscous flows for $\alpha=4°$ and $Re=10^4$. A stabilized finite element method based on the SUPG/PSPG stabilizations has been used to solve, both, flow and adjoint equations. The results of an experimental investigation of the heat transfer coefficients for forced convection from a NACA-63421 airfoil are presented by Wang et al. [3]. Wind tunnel measurements of convection coefficients are obtained for air flow temperatures from 20 to 30°C. The experimental data are correlated with respect to the Nusselt and Reynolds numbers. Both average and spatial variations of the heat transfer coefficients are non-dimensionalized through modifications of a classical Hilpert correlation for cylinders in crossflow. Henriques et al. [4] showed that a pressure-load inverse design method was successfully applied to the design of a high-loaded airfoil for application in a small wind turbine for urban environment. Predescu et al. [5] described the experimental work in a wind tunnel on wind turbine rotors having different number of blades and different twist angle. The aim of the work is to study the effects of the number of blades, the blade tip angles and twist angle of the blades on the power coefficient of the rotor. Sicot et al. [6] investigated the aerodynamic properties of a wind turbine airfoil. Particularly, they studied the influence of the inflow turbulence level (from 4.5% to 12%) and of the rotation on the stall mechanisms in the blade. A

local approach was used to study the influence of these parameters on the separation point position on the suction surface of the airfoil, through simultaneous surface pressure measurements around the airfoil. Schreck and Robinson [7] showed that wind turbine blade aerodynamic phenomena can be broadly categorized according to the operating state of the machine, and two particular aerodynamic phenomena assume crucial importance. At zero and low rotor yaw angles, rotational augmentation determines blade aerodynamic response. At moderate to high yaw angles, dynamic stall dominates blade aerodynamic. Hu et al. [8] showed that Coriolis and centrifugal forces play important roles in 3D stall-delay. At the root area of the blade, where the high angles of attack occur, the effect of the Coriolis and centrifugal forces is strong. Thus, it shows apparent stall-delay phenomenon at the inner part of the blade. However, by increasing the Reynolds number, the separation position has a stronger effect than by increasing the Coriolis and centrifugal forces. Wright and Wood [9] showed that the acceleration and deceleration of the rotor at speeds below its controlled maximum speed, and for a range of wind speeds was calculated and compared with data. Hirahara et al. [10] showed that a unique and very small wind turbine, mF500 with 500 mm diameter and small aspect ratio was developed for wide use in urban space. The basic performance of μF500 was tested for various free stream and load resistance. The airflow around the turbine was investigated by using a particle image velocimetry (PIV). The main goal of the Mirzaei et al. [11] investigation was to understand the flow field structure of the separation bubble formed on NLF-0414 airfoil with glaze-ice accretions using CFD and hot-wire anemometry and comparing these results with previous researches performed on NACA 0012 airfoil. Based on previous results studying the horizontal axis NACA2415 airfoil type wind turbine is needed.

In this paper, we are interested in studying the aerodynamic characteristics of a NACA2415 airfoil type horizontal axis wind turbine to gain an insight into the complex flow field developing around a small incurved wind rotor and to evaluate its performance. The experimental results are also presented in order to validate the numerical results computed by a computational fluid dynamics Code "SolidWorks Flow Simulation". A good agreement between the numerical and experimental results is obtained which confirms the validity of the adopted method.

2. Numerical Model

In this work, we are interested in studying the NACA2415 airfoil wind turbine with a wedging angle equal to β=30° (figure 1). In these conditions, the multi reference approach has been used. Which consists on using a rotating area with a diameter D=373 mm and a length L= 410 mm (figure 2). The boundary conditions used are summarized in figure 3. In these conditions, the velocity inlet is equal to V=3 m.s^{-1}, the pressure outlet equal to p=101325 Pa and the angular velocity is equal to Ω=42 rad.s^{-1}.

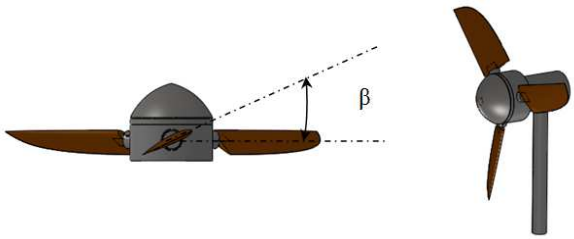

Fig. 1. *Wind turbine.*

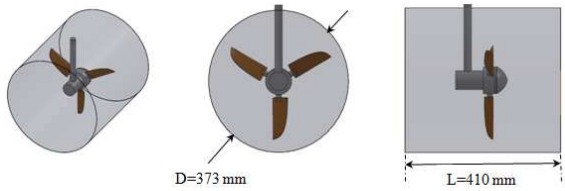

Fig. 2. *Rotating area.*

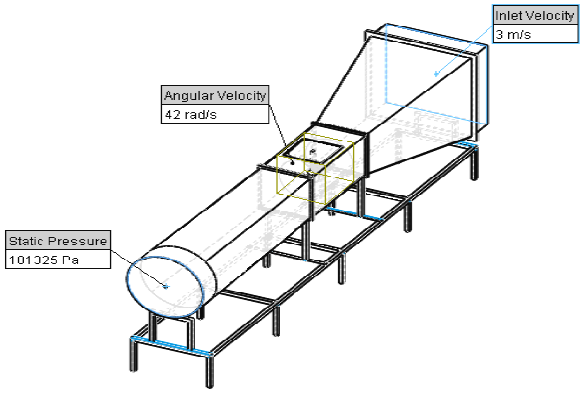

Fig. 3. *Boundary conditions.*

3. Results and Discussions

In this section, we will study the local characteristics at different compliance planes defined by x=0mm, y=0 mm, z=0 mm, z=50 mm, z=-50 mm and z=-100 mm (figure 4).

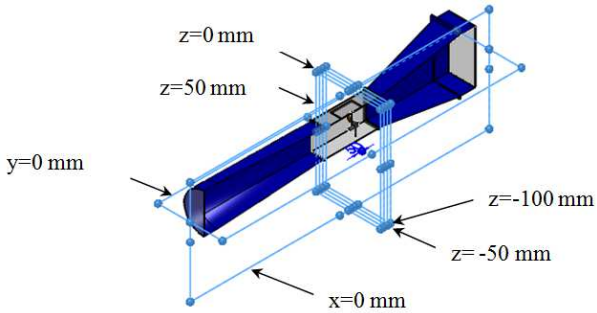

Fig. 4. *Compliance planes.*

3.1. Velocity Fields

Figures 5 and 6 show the distribution of the velocity vectors in different longitudinal and transverse planes in the

rotating area limeted by x=0mm, y=0 mm, z=0 mm, z=50 mm, z=-50 mm and z=-100 mm. The results show that, the wind turbine has a direct effect on the velocity vectors distribution near the rotating area. If fact, when crossing the wind turbine, a flow deflection has been observed. At level of blades, an acceleration of the flow occured. In addition, two recirculation zones occured at the level of the wind turbine cover and in the wind turbine downstream.

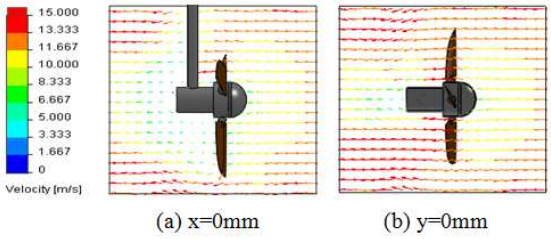

Fig. 5. *Velocity fields in the longitudinal planes.*

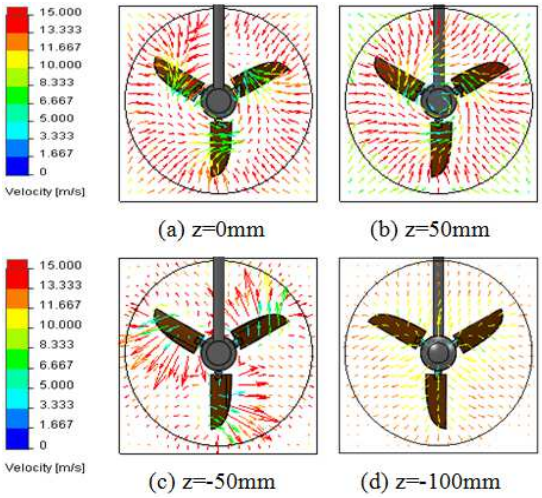

Fig. 6. *Velocity fields in the transverse planes.*

3.2. Average Velocity

Figure 7 shows the distribution of the average velocity in the different longitudinal defined by x=0 mm and y=0 mm. According to these results, the wind turbine has a direct effect on the distribution of the average velocity. In fact, two large wakes, characteristic of the maximum values of the velocity average, are developed at the level of blades. However, two others wakes are developed. The first one has been observed at the level of the cover and the second is observed in the wind turbine downstream. The lowest value is obtained in the wind turbine downstream.

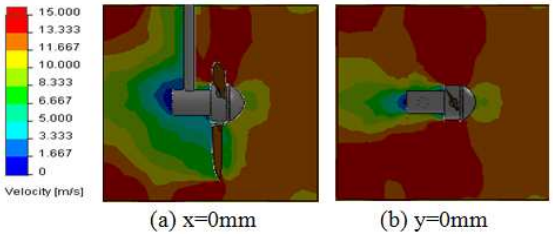

Fig. 7. *Average velocity distribution in the longitudinal planes.*

3.3. Static Pressure

Figure 8 shows the distribution of the static pressure in the rotating area in the longitudinal planes defined by x=0 mm and y=0 mm. According to these results, the wind turbine has a direct effect on the distribution of the static pressure. In fact, a compression zone has been observed in the wind turbine upstream and a depression zone in the wind turbine downstream. The static pressure attains its minimum value in the blades downstream.

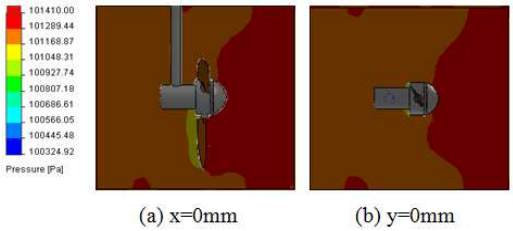

Fig. 8. *Static pressure distribution in the longitudinal planes.*

3.4. Dynamic Pressure

Figure 9 shows the distribution of the dynamic pressure in the rotating area in the longitudinal planes defined by x=0 mm and y=0 mm. According to these results, the wind turbine has a direct effect on the distribution of the dynamic pressure. In fact, a compression zone has been observed in the wind turbine upstream and a depression zone in the wind turbine downstream.

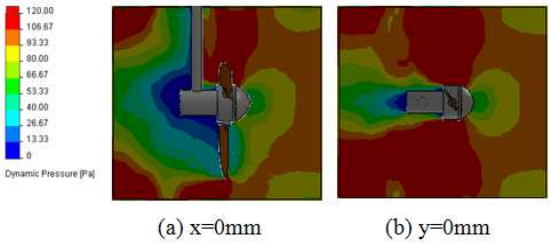

Fig. 9. *Dynamic pressure distribution in the longitudinal planes.*

3.5. Turbulent Kinetic Energy

Figure 10 shows the distribution of the turbulent kinetic energy in the rotating area in the longitudinal planes defined by x=0 mm and y=0 mm. According to these results, the wind turbine has a direct effect on the distribution of the turbulent kinetic energy. In fact, maximum value of the characteristic of the turbulent kinetic energy is developed around the wind turbine.

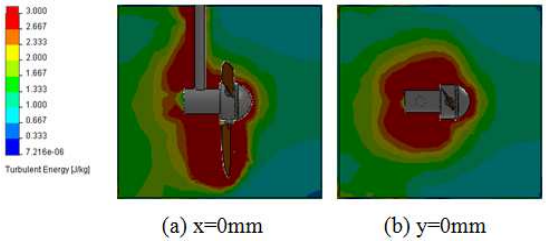

Fig. 10. *Distribution of the turbulent kinetic energy in the longitudinal planes.*

3.6. Dissipation rate of the Turbulent Kinetic Energy

Figure 11 shows the distribution of the dissipation rate of the turbulent kinetic energy in the rotating area at different longitudinal planes defined by x=0 mm and y=0 mm. According to these results, the wind turbine has a direct effect on the distribution of the dissipation rate of the turbulent kinetic energy. In fact, a wake, characteristic of the maximum value of the dissipation rate of the turbulent kinetic energy, is developed around the wind turbine.

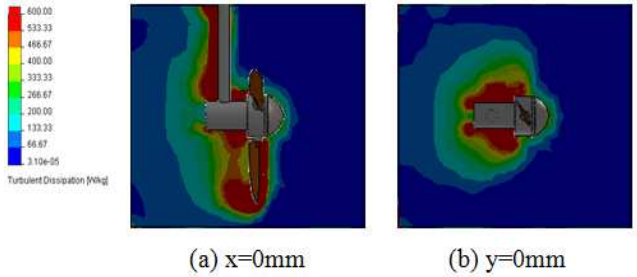

Fig. 11. *Dissipation rate of the turbulent kinetic energy in the longitudinal planes.*

3.7. Turbulent Viscosity

Figure 12 shows the distribution of the turbulent viscosity in the rotating area at different longitudinal planes defined by x=0 mm and y=0 mm. According to these results, the wind turbine has a direct effect on the distribution of the turbulent viscosity. In fact, a wake, characteristic of the highly turbulent viscosity, is developed in the wind turbine upstream.

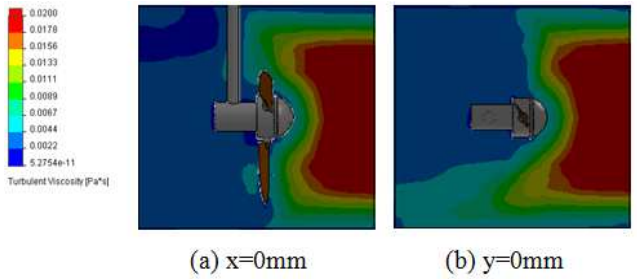

Fig. 12. *Turbulent viscosity distribution in the longitudinal planes.*

3.8. Vorticity

Figure 13 shows the distribution of the vorticity in the rotating area at different longitudinal planes defined by x=0 mm and y=0 mm. According to these results, the wind turbine has a direct effect on the distribution of the vorticity. In fact, a wake, characteristic of the highly vorticity, is developed around the wind turbine. However, it has been noted that this wake becomes more limited and located around the wind turbine, especially, in the blades downstream.

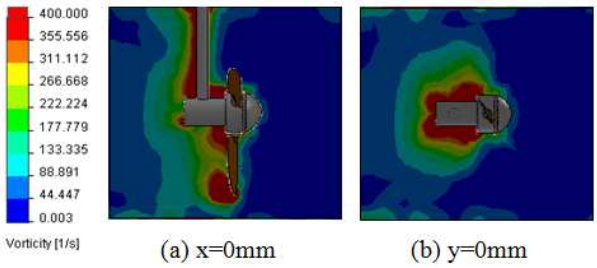

Fig. 13. *Vorticity distribution in the longitudinal planes.*

4. Experimental Validation

Figure 14 shows the velocity profiles in the transverse plane defined by z=50 mm. This plane is studied in the test section of the wind tunnel downstream of the wind turbine. These profiles corresponds to x=0 mm, x=50 mm, x=100 mm, x=150 mm, x=-50 mm, x=-100 mm, respectively. The numerical results show a good agreement with experimental results. This confirms that our numerical model is capable of predicting the aerodynamic characteristics of the airflow around the wind turbine.

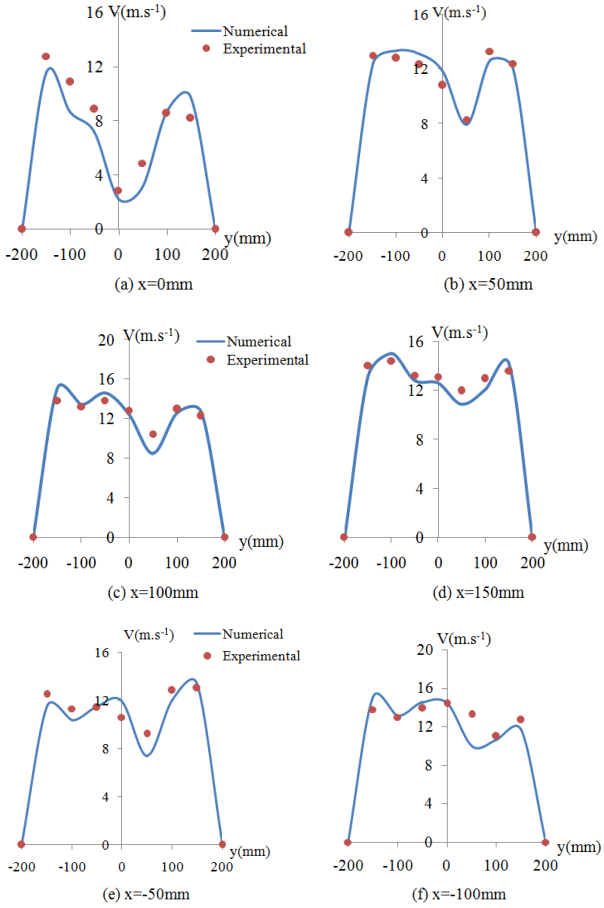

Fig. 14. *Velocity profile in the plane z=50 mm.*

5. Conclusions

In this paper, we have achieved a fluid dynamic study of a

NACA2415 airfoil type wind turbine with a wedging angle equal to 30° in a dynamic state. Also, we are interested in measuring the average velocity of the flow at different locations in the test vein. The good agreement between numerical and experimental results confirms the validity of the numerical method. In the future, we propose to extend the study to others geometrical parameters.

References

[1] L. Leifsson, S. Koziel, Multi-fidelity design optimization of transonic airfoils using physics-based surrogate modeling and shape-preserving response prediction, Journal of Computational Science 1 (2010) 98-106.

[2] D.N. Srinath, S. Mittal, Optimal aerodynamic design of airfoils in unsteady viscous flows, Computer Methods in Applied Mechanics and Engineering 199 (2010) 1976-1991.

[3] X. Wang, E. Bibeau, G.F. Naterer, Experimental correlation of forced convection heat transfer from a NACA airfoil, Experimental Thermal and Fluid Science 31 (2007) 1073-1082.

[4] J.C.C. Henriques, F. Marques da Silva , A.I. Estanqueiro, L.M.C. Gato, Design of a new urban wind turbine airfoil using a pressure-load inverse method, Renewable Energy 34 (2009) 2728-2734.

[5] M. Predescu, A.Bejinariu, O.Mitroi, A. Nedelcu, Influence of the Number of Blades on the Mechanical Power Curve of Wind Turbines, International Conference on Renewable Energies and Power Quality (2009).

[6] C. Sicot, P. Devinant, S. Loyer, J. Hureau, Rotational and turbulence effects on a wind turbine blade. Investigation of the stall mechanisms, Journal of Wind Engineering and Industrial Aerodynamics 96 (2008) 1320-1331.

[7] S.J. Schreck and M.C. Robinson, Horizontal Axis Wind Turbine Blade Aerodynamics in Experiments and Modeling, IEEE Transactions on Energy Conversion, 22 (2007) 61-70.

[8] D. Hu, O. Hua, Z. Du, A study on stall-delay for horizontal axis wind turbine, Renewable Energy 31 (2006) 821-836.

[9] A.K. Wrigh, D.H. Wood, The starting and low wind speed behaviour of a small horizontal axis wind turbine, Journal of Wind Engineering and Industrial Aerodynamics 92 (2004) 1265-1279.

[10] H. Hirahara, M. Zakir Hossain, M. Kawahashia, Y. Nonomura, Testing basic performance of a very small wind turbine designed for multi-purposes, Renewable Energy 30 (2005) 1279-1297.

[11] M. Mirzaei, M.A. Ardekani, M. Doosttalab, Numerical and experimental study of flow field characteristics of an iced airfoil, Aerospace Science and Technology, 13,(2009) 267-27.